


 Cite this: *RSC Adv.*, 2018, **8**, 21480

Development, modification, and application of low-cost and available biochar derived from corn straw for the removal of vanadium(v) from aqueous solution and real contaminated groundwater[†]

 Ruihong Meng,^{ab} Tan Chen,^c Yixin Zhang,^d Wenjing Lu,^{*ab} Yanting Liu,^{ab} Tianchu Lu,^e Yanjun Liu^{ab} and Hongtao Wang^{*ab}

In this work, a low-cost and available material for use as a permeable reactive barrier (PRB) to prevent vanadium in groundwater from leaking into river water was developed. Three modified biochars were prepared from available corn straw pretreated with CsCl, Zn(II), and Zr(IV) to enhance ion exchange capacity (IEC) and specific surface area, and were designated as Cs-BC, Zn-BC, and Zr-BC, respectively. These materials were characterized via IEC, N₂ adsorption-desorption, Fourier-transform infrared spectroscopy (FTIR), and X-ray diffraction (XRD) analyses. The Langmuir isotherm model could be applied for the best fit for the adsorption data of Cs-BC and Zr-BC, indicating that vanadium(v) sorption occurred in a monolayer. The vanadium(v) adsorption capacities of Cs-BC, Zn-BC, and Zr-BC were 41.07, 28.46, and 23.84 mg g⁻¹, respectively, which were 3.22–5.55 times higher than that of commercial activated carbon (AC) (7.40 mg g⁻¹), probably because of their higher IECs and specific surface areas after modification. In addition, no heavy metal leaching was found from the modified biochars during the adsorption processes when pH > 2. According to the FTIR and XRD patterns, the adsorption mechanism of Cs-BC and Zr-BC was ion exchange, whereas for Zn-BC, it was mainly surface precipitation and electrostatic attraction. The adsorption of vanadium(v) onto the modified biochars was independent of pH in the range of 4.0 to 8.0. Furthermore, the removal efficiency of the vanadium(v) in real contaminated groundwater from the catchment of the Chaobei River by Zn-BC reached 100% at a dose of 4 g L⁻¹. Hence, modified biochars are promising PRB filling materials for removing vanadium(v) from contaminated groundwater.

Received 12th March 2018
 Accepted 4th June 2018

DOI: 10.1039/c8ra02172d
rsc.li/rsc-advances

Introduction

Mining and smelting of vanadium have caused widespread pollution in many countries, such as Russia, South Africa, and China.¹ High concentrations of vanadium have been observed in the groundwater around smelting and mining areas. For instance, the total average concentration of vanadium in shallow groundwater near the slag field of the Baguan River in the Panzhihua area has been reported as 13.98 mg L⁻¹,² and the

unfiltered water of the Yangtze River has had reported vanadium concentrations from 0.24 to 64.5 µg L⁻¹.³ The area we studied is located in the catchment of the Chaobei River, which is a branch of the Hanjiang River, in Hebei province (Fig. 1). The Hanjiang River is the main tributary of the Danjiangkou Reservoir, which is the water source for the Middle Route of the South-to-North Water Transfer Project (MR-SNWTP) of China, one of the largest infrastructural projects in China, with the goal of diverting water to Tianjin, Beijing, and other northern cities along the route. In the Chaobei River catchment, a tailings site of a local vanadium smelter is located 1.3 kilometres away from the river. High concentrations of vanadium (15–1817 mg kg⁻¹), chromium (19–1183 mg kg⁻¹), and copper (20–456 mg kg⁻¹) were detected in the soils of the vanadium tailings site,⁴ which significantly exceed the soil guidelines (130 mg kg⁻¹ for vanadium, 200 mg kg⁻¹ for chromium, and 200 mg kg⁻¹ for copper) of the Chinese Environmental Quality Standard for Soils (GB15618-2008). Leaching from the contaminated soil and vanadium tailings at this site led to high accumulation of vanadium in the groundwater recharging to the Chaobei River.

^aSchool of Environment, Tsinghua University, Beijing 100084, P. R. China. E-mail: htwang@tsinghua.edu.cn; luwenjing@tsinghua.edu.cn

^bKey Laboratory for Solid Waste Management and Environment Safety, Ministry of Education of China, Tsinghua University, Beijing 100084, P. R. China

^cCollege of Life and Environmental Sciences, Minzu University of China, Beijing 100081, P. R. China

^dCollege of Environmental Science and Engineering, Hunan University, Changsha 410082, P. R. China

^eCECEP Clean Technology Development Co., Ltd, Beijing 100083, P. R. China

[†] Electronic supplementary information (ESI) available. See DOI: [10.1039/c8ra02172d](https://doi.org/10.1039/c8ra02172d)



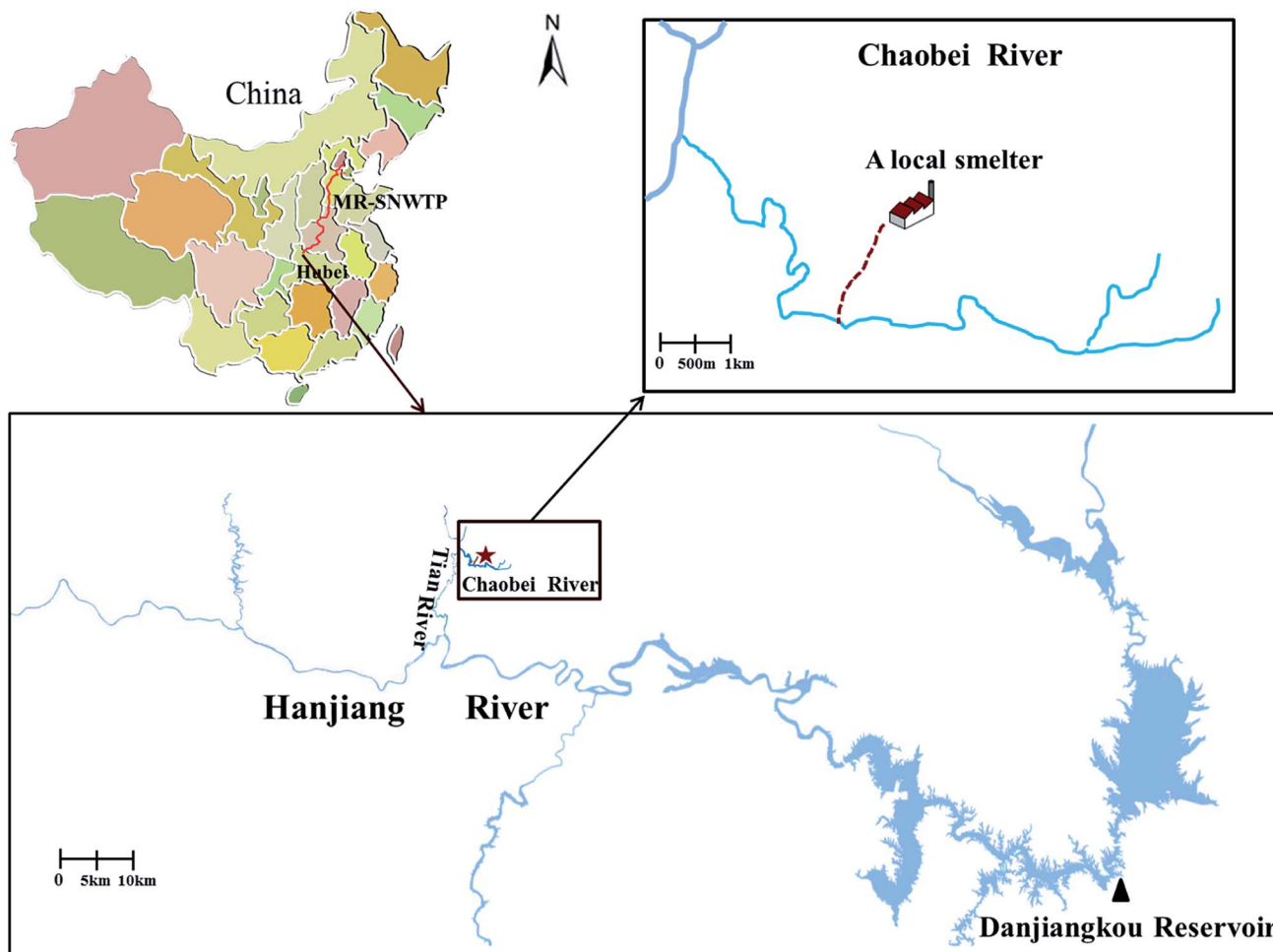


Fig. 1 Middle Route of the South-to-North Water Transfer Project (MR-SNWTP) and Danjiangkou Reservoir and its tributaries.

The vanadium concentrations of groundwater detected in the study area were in range of $1\text{--}11\text{ mg L}^{-1}$, which is 20 to 220 times higher, respectively, than the water standard (0.05 mg L^{-1}) according to both the China's drinking water standard (GB 5749-2006) and the California Department of Public Health's drinking water standard.⁵ Vanadium has various valence states, *e.g.* +3, +4, and +5, with vanadium(v) the most common state, which is present as a vanadate oxyanion (*e.g.* VO_4^{3-} , VO_3^- , H_2VO_4^- and HVO_4^{2-}). As vanadium(v) exists in anionic form in aqueous solutions, it is more difficult to capture than metal cations are. Therefore, it is crucial to prevent the tailing site pollutants entering the river.

In the groundwater recharge area of the Chaobei River, leachate from the tailings site, which has a high concentration of vanadium, flows down a gully toward the Chaobei River and along the way infiltrates the groundwater, which recharges the river. An effective approach for stopping the vanadium from reaching the river is to build a permeable reactive barrier (PRB) before the groundwater flow into the river. PRBs generally contain reactive materials that remove contaminants through biological, physical and/or chemical processes, as the contaminants remain inside the reactive materials.⁶⁻⁸ Vanadium(v) cannot be removed effectively by commercial activated carbon

(AC), which is the most commonly used reactive material, because of its low adsorption capacity, narrow optimum pH range, and low adaptability to wide-ranging vanadium(v) wastewaters. In previous studies, ZnCl_2 activated carbon,⁹ protonated chitosan flakes,¹⁰ metal (hydr)oxide adsorbents,¹¹ goethite ($\alpha\text{-FeOOH}$),¹² ZrOCl_2 -loaded orange juice residue¹³ and calcined Mg/Al hydrotalcite were reported to have potential abilities to remove vanadium(v) from aqueous solution. Although the metal (hydr)oxide adsorbents and calcined Mg/Al hydrotalcite had high adsorption capacities, they are too expensive for practical application in treating contaminated groundwater. Therefore, a low-cost and available adsorbent needs to be developed for the removal of vanadium(v) from the contaminated sites.

Biochar, as a potential adsorbent material, is a product of thermal pyrolysis of carbon-rich biomass in an oxygen-deficient environment.¹⁴ Using biochars derived from agricultural waste for the removal of the heavy metal ions provides an economical and environmentally friendly alternative to commercial ACs. Corn straw (CS), a kind of renewable biomass, is widely available and low-cost valuable raw material for biochar production, as it has abundant carbon components. Additionally, over 250 million tons of CS are generated annually in China,^{15,16} most of

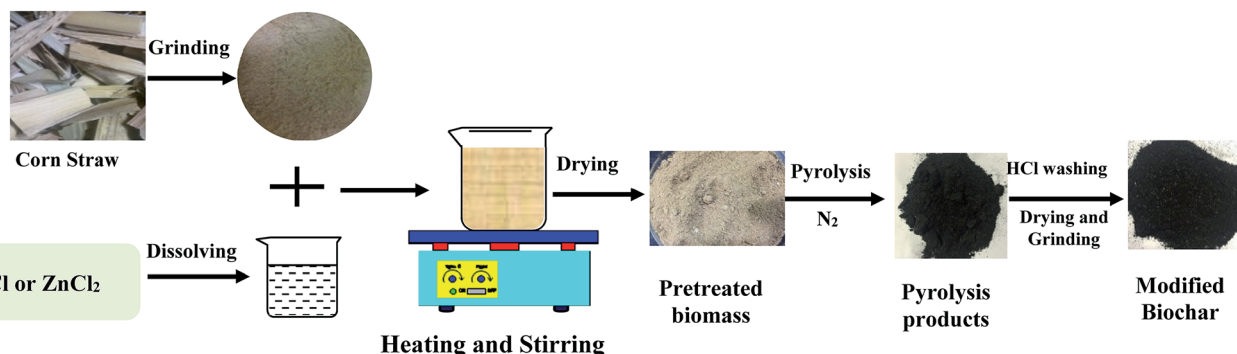


Fig. 2 Preparation of modified biochars from corn straw.

which are burnt in the field, resulting in serious air pollution. A few studies have reported the application of biochars obtained *via* fast pyrolysis, for instance, oak bark, energy cane, and wood biochars, were used to successfully remove arsenic, lead, fluoride, chromium, and cadmium during water purification.^{17–19} However, the structure of the biochar generated this way is possibly underdeveloped owing to the short residence time of the fast pyrolysis process, thereby influencing its full potential application as an absorbent. Surface chemical characteristics and porosity are critical factors that greatly influence the adsorption performance of biochars. Therefore, various methods including surface modifications, activation, and hydrothermal synthesis have been developed, which result in cost-efficient biochars with high adsorption capacities that are comparable to or even exceed AC capabilities.¹⁹ Chemical modifications of biochars are widely applied, mainly using the reagents citric acid,²⁰ KOH,²⁰ KMnO₄,²¹ and ZnCl₂ (ref. 22) to impregnate the raw feedstock, which influence their pyrolytic decomposition. Among these reagents, ZnCl₂ is considered a less expensive and more effective agent for producing modified biochar. ZnCl₂ impregnation could significantly increase the generation of mesopores and micropores, the specific surface area, and the yields of biochar.^{23–26} Recently, transitional Zr(IV)-binding chitosan complexes, orange waste gel and AC have been applied for the removal of phosphate,^{27,28} As(V) and As(III),^{29,30} Cr(VI) and vanadium(V),^{13,31,32} because hydrous Zr(IV) can form tetrahedral geometries with abundant water molecules and hydroxyl ions, which could give rise to adsorption sites and high adsorption affinity toward oxyanions. Moreover, Zr(IV) in its hydrated form can resist the adsorption of alkalis, acids, reductants and oxidants, which can improve the selectivity of the absorbents. Thus, biochar derived from CS that has been modified with Zr(IV) and Zn(II) in order to remove vanadium(V) from real contaminated groundwater might offer a simple, low-cost and efficient approach. Additionally, there have been no reports of the adsorption capacities and mechanisms of vanadium(V) interaction related to Zr(IV)- and Zn(II)-modified biochar derived CS.

The aim of the present work was to find a low-cost and available biochar that could be used as a reactive material in a PRB for the removal of vanadium from contaminated groundwater in the catchment of the Chaobei River. To obtain

a biochar for the efficient removal of vanadium(V), many kinds of feedstocks, including CS, wheat straw, peanut shell, corncob, shrub and *Spirogyra* were used for the biochar production. The behaviours of vanadium(V) adsorption onto the modified biochars derived from CS pretreated with ZnCl₂, CsCl and Zr(SO₄)₂ were investigated *via* batch experiments. To analyse the mechanisms of vanadium adsorption onto modified biochars, the modified biochars were characterized using Fourier transform infrared (FT-IR) spectroscopy and X-ray diffraction (XRD) before and after the adsorption.

Material and methods

Materials

All chemicals used in this study were analytically pure. NH₄VO₃, CsCl, HCOOH, ZnCl₂ and Zr(SO₄)₂ were acquired from Tianjin Guangfu Fine Chemical Research Institute, China. The raw material of CS, wheat straw, peanut shells, and corncobs were collected from a suburb of Xinle City, Hebei province, China. The raw materials of shrubs, *Spirogyra*, and cinder residue were collected from a suburb of Yunxi County, Shiyan City, Hubei province, China. Zeolite, bentonite, and AC were purchased

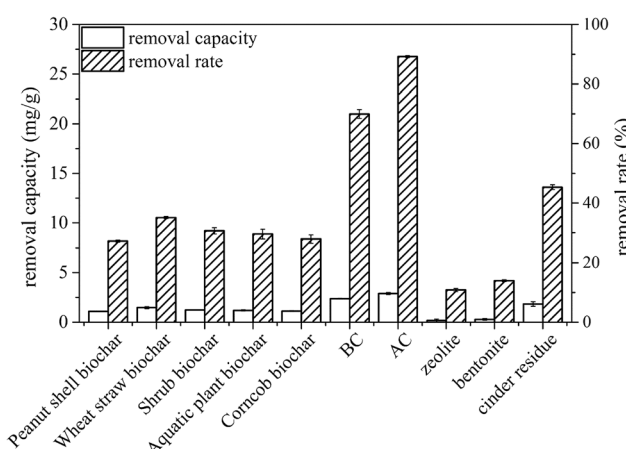


Fig. 3 Removal of vanadium(V) by biochars and commercial materials. Equilibrium conditions: adsorbent dosage, 4 g L⁻¹; 25.0 ± 1.0 °C; initial concentration, 50 mg L⁻¹.



Table 1 Main properties of the modified biochars, BC, and AC

| Parameter | Cs-BC | Zn-BC | Zr-BC | BC | AC |
|---|--------------|--------------|--------------|--------------|--------------|
| Yield percentage (wt%) | 33.60 ± 0.29 | 34.01 ± 0.58 | 31.25 ± 0.40 | 27.46 ± 0.69 | |
| Ash content percentage (wt%) | 13.31 ± 0.91 | 13.54 ± 0.37 | 51.03 ± 0.30 | 20.55 ± 0.33 | 9.85 ± 0.31 |
| Elemental analysis/wt% | | | | | |
| C | 70.92 ± 0.17 | 75.72 ± 0.55 | 40.15 ± 1.05 | 67.22 ± 0.19 | 83.91 ± 0.47 |
| H | 1.80 ± 0.07 | 1.59 ± 0.04 | 1.45 ± 0.06 | 1.76 ± 0.11 | 1.98 ± 0.05 |
| O | 9.01 ± 0.07 | 5.69 ± 0.15 | 13.34 ± 0.07 | 7.48 ± 0.04 | 6.03 ± 0.24 |
| N | 0.69 ± 0.19 | 0.99 ± 0.02 | 0.86 ± 0.02 | 1.08 ± 0.02 | 0.56 ± 0.14 |
| Atomic ratio | | | | | |
| C + H + O + N | 82.42 | 83.99 | 55.80 | 77.54 | 92.49 |
| H/C | 0.025 | 0.021 | 0.036 | 0.026 | 0.024 |
| O/C | 0.127 | 0.075 | 0.332 | 0.111 | 0.072 |
| (N + O)/C | 0.137 | 0.088 | 0.354 | 0.127 | 0.078 |
| pH (S/L = 1 : 10) | 7.06 | 6.64 | 10.51 | 9.49 | 7.42 |
| pH _{PZC} | 6.89 | 6.53 | 10.03 | 9.25 | 7.07 |
| IEC (cmol kg ⁻¹) | 237.26 | 54.18 | 201.49 | 86.51 | 126.10 |
| Cesium content (mmol g ⁻¹) | 0.36 | | | | |
| Zinc content (mmol g ⁻¹) | | 0.48 | | | |
| Zirconium content (mmol g ⁻¹) | | | 1.26 | | |

from Shanghai Aladdin Biological Technology Co., Ltd, China, and sieved through a 0.45 mm mesh.

Preparation of modified biochars

The raw CS, wheat straw, peanut shells, corncobs, shrubs, and *Spirogyra* were air-dried for 72 h and then heated at 80 °C until the weight was constant. The dried CS, wheat straw, peanut shells, corncobs, shrubs, and *Spirogyra* were smashed and sieved to obtain a particle size of 40 mesh (0.45 mm) for further chemical modification.

The biochars were prepared *via* fast pyrolysis in a tube furnace according to the method reported by Chen *et al.*³³ The fast pyrolysis was conducted at 700 °C with N₂ as internal shielding gas. The raw materials (CS, wheat straw, peanut shells, corncobs, shrubs and *Spirogyra*) were kept in heating area for 0.5 h. The resulting biochars were sieved to obtain particles from 40 mesh (0.45 mm). The biochar derived from CS was designated as BC.

As the objective of this work was to develop a low-cost PRB filling material, considering the costs of the reagents, the weight ratios of reagents to CS were 1 : 10, 1 : 2, and 1 : 1.5 for CsCl, ZnCl₂ and Zr(SO₄)₂, respectively.

CsCl-modified biochar (Cs-BC) and Zn(II)-modified biochar (Zn-BC) were prepared according to the following procedures.⁹ By dissolving 10 g of CsCl in 500 mL of deionized water, a 20 g L⁻¹ CsCl solution was prepared. By dissolving 50 g of ZnCl₂ in 500 mL of deionized water, a 100 g L⁻¹ ZnCl₂ solution was prepared. As shown in Fig. 2, 100 g of dried CS was added into 500 mL of the 20 g L⁻¹ CsCl solution or 100 g L⁻¹ ZnCl₂ solution and stirred for 4 h at 100 °C, resulting in CsCl- or Zn(II)-impregnated CS, respectively. The two impregnated CSs were filtered and then dried at 70 °C for 24 h. Subsequently, they were carbonized at 700 °C according to the fast pyrolysis process described above. As the carbonized materials cooled, the excess reagents (CsCl or Zn(II)) retained in the products were leached out using 1% HCl. The samples were washed several times with deionized water to get rid of traces of HCl and the reagents

(CsCl or Zn(II)). Then, they were dried at 105 °C for 24 h and then sieved through 40 mesh (0.45 mm). Finally, Cs-BC and Zn-BC were obtained.

Zr(IV)-impregnated CS was prepared in accordance with the procedures described by Liao *et al.*³⁴ First, 30 g CS was added to 400 mL of designed solution with a pH value between 1.7 and 2.0 for 24 h. Then, 20 g of Zr(SO₄)₂ was added, and the mixture was stirred for 4 h at 30 °C. After this, we gradually added NaHCO₃ solution (15% w/w) over 2 h, until the desired pH between 4.0 and 4.5 was reached, after which, the reaction was continued for another 4 h at 40 °C. After impregnation, the Zr(IV)-impregnated CS was collected *via* filtration, washed with deionized water and finally dried at 70 °C for 24 h. The product was carbonized at 700 °C according to the fast pyrolysis process described above. The carbonized material was sieved to obtain a particle size of 40 mesh. Finally, Zr-BC was obtained.

Characteristics of the modified biochars

The samples were calcinated at 650 °C for 2 h in a muffle furnace, and the remaining mass percentage of the samples was considered the ash content. The elemental contents of C/H/O/N were determined using an elemental analyser (EA3000, Euro-Vector, Italy). Samples were added to deionized water at a maximum ratio of 1 : 10 (w/v), and a pH meter (FE20, Mettler-Toledo, Switzerland) was used to measure the sample pH. The pH_{PZC} of the absorbents was measured in accordance with the procedures described by Mahmood *et al.*³⁵ The cobalt hexamine

Table 2 Microstructure properties of the modified biochars, BC, and AC

| Parameter | Cs-BC | Zn-BC | Zr-BC | BC | AC |
|---|--------|--------|-------|-------|--------|
| BET surface area (m ² g ⁻¹) | 108.31 | 150.36 | 85.58 | 27.45 | 735.63 |
| Pore size (nm) ^a | 1.43 | 1.44 | 1.44 | 1.41 | 1.43 |
| Pore volume (cm ³ g ⁻¹) ^b | 0.064 | 0.089 | 0.075 | 0.024 | 0.458 |

^a Barrett, Joyner, and Halenda model, desorption data. ^b P/P₀ = 0.98.



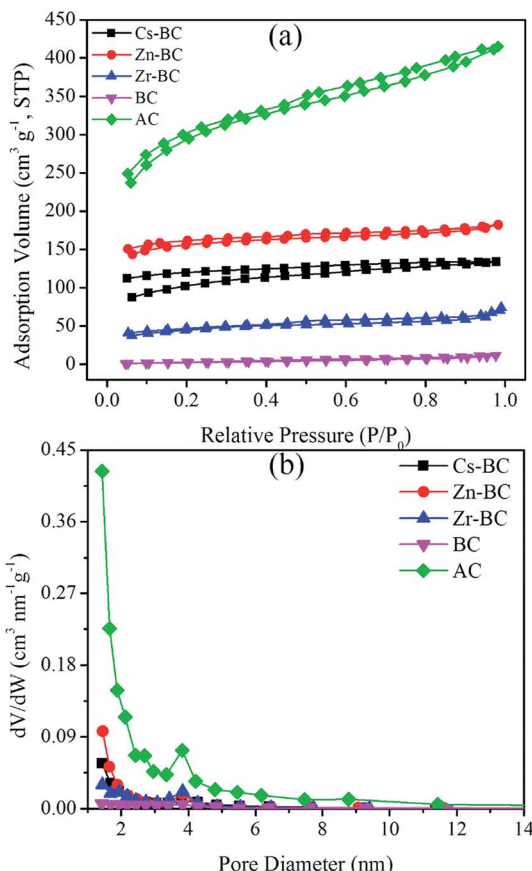


Fig. 4 Surface characteristics of the modified biochars, BC, and AC. (a) N₂ adsorption–desorption isotherms; (b) pore size distribution curves.

ion exchange approach, as reported by Hu *et al.*,³⁶ was used to determine the ion exchange capacity (IEC) of the adsorbents. The heavy metal concentration was determined *via* ICP-OES (Prodigy7, Leeman Labs, USA).

The pore characteristics and surface area of the adsorbents were measured by the N₂ adsorption–desorption isotherm with a gas sorption apparatus (Autosorb-1-C, Quantachrome, USA). The samples were degassed at 300 °C prior to measurement. The micromorphology of all the adsorbents was observed by a JSM-6301F scanning electron microscope (SEM, Hitachi, Japan). The thermogravimetric (TG) curves were obtained from a TG system (STA 409C, NETZSCH, Germany), at a heating rate of 10 °C min⁻¹ from 38 °C to 1000 °C, and under N₂ with flow rate of 20 mL min⁻¹.

Crystalline structure was analysed through XRD with an X-ray diffractometer (D8 ADVANCE, Bruker, Germany), which was operated at 40 mA and 40 kV under Cu K α radiation. Characteristic functional groups in the adsorbents were analysed through FTIR spectroscopy (Spectrum GX, Perkin Elmer, USA), with wave numbers in the region of 4000–400 cm⁻¹. OMNIC 8.2 software (Thermo Scientific, USA) was used in spectrogram smoothing, baseline correction, and standardization of the original data.

Adsorption experiments

2.4.1 Vanadium adsorption experiments. The desired vanadium(v) solutions of 5, 10, 20, 50, 100, and 250 mg L⁻¹ were prepared by dissolving NH₄VO₃ in deionized water. The initial pH of the vanadium(v)-bearing solutions was not adjusted before adsorption.

Adsorption batch experiments were carried out by mixing 25 mL of the desired concentration of vanadium(v) aqueous solution with 25 mg of modified biochar in a vortex maker for 48 h at 200 rpm and 25 °C. Test adsorbents included modified biochars and BC, with AC employed as a control. In the adsorption experiments, dosages of the modified biochars, BC and AC were 1 g L⁻¹, 8 g L⁻¹, and 8 g L⁻¹, respectively. All adsorption experiments were conducted in triplicate, and the initial solution was determined as the blank control. At the end of the adsorption, we filtered the residual solution with a 0.45 μ m membrane. Finally, the vanadium(v) solution concentrations were measured *via* ICP-OES (Prodigy7, Leeman Labs, USA). The adsorption capacity q_e (mg g⁻¹) and removal efficiency (%) of the adsorbents were calculated using the following equations:

$$q_e = (C_0 - C_e)V/m \quad (1)$$

$$\text{Removal efficiency}(\%) = (C_0 - C_e) \times 100/C_0 \quad (2)$$

where C_0 and C_e are the initial and equilibrium concentrations of the vanadium(v) solution (mg L⁻¹), respectively; V is the solution volume (mL); and m is the weight of the adsorbent used (mg).

2.4.2 Effect of pH. The effect of pH in the range 2.0–11.0 on the removal of vanadium(v) from aqueous solution was investigated. The pH of the vanadium(v) solution, which was determined by a pH meter (FE20, METTLER TOLEDO, Switzerland), was adjusted with 0.01 M NaOH solutions and 0.01 M HNO₃. The dose of an adsorbent used was 1 g L⁻¹ with the initial vanadium(v) concentration of 50 mg L⁻¹. The adsorption procedures were referred to those in Section 2.4.1.

Results and discussion

Removal of vanadium(v) by biochars and commercial materials

Fig. 3 shows the removal of vanadium(v) by the biochars derived from different feedstocks and commercial materials. All the biochars showed different adsorption abilities, which is reflected by the following sequence of the vanadium(v) adsorption capacity: BC > wheat straw biochar > shrub biochar > *Spirogyra* biochar > corncob biochar > peanut shell biochar. Compared with the commercial materials, BC showed higher removal efficiency than zeolite, bentonite, and cinder residue, but a little lower removal efficiency than that of AC (27.5%). These results suggest that the biochar derived from CS have the potential to remove vanadium(v) from aqueous solution. As the removal efficiency was still low, to improve the adsorption capacity of BC, CS was pretreated with chemicals to obtain modified biochars.



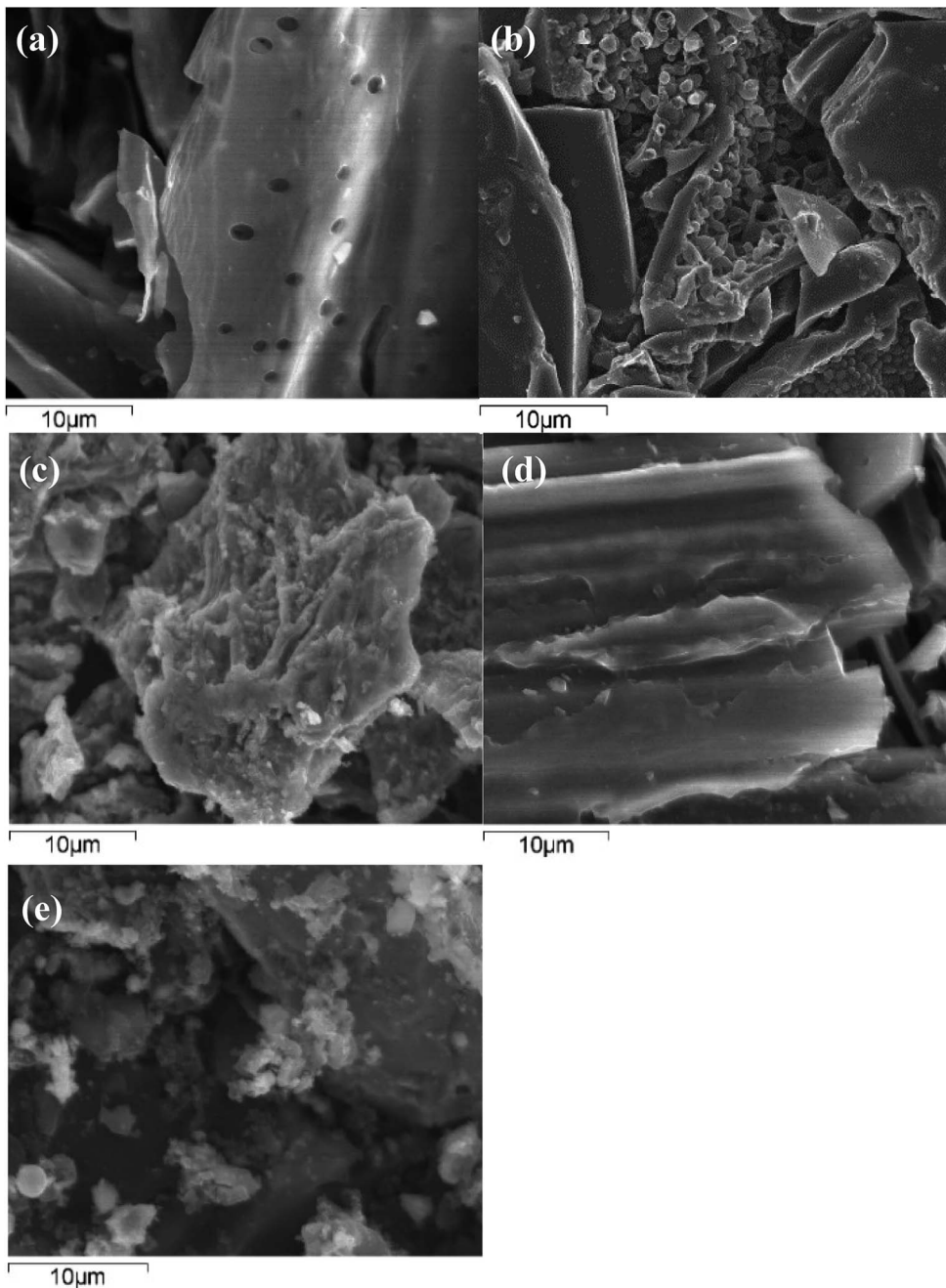


Fig. 5 SEM images (3000 \times magnification) of modified biochars, BC, and AC: (a) Cs-BC, (b) Zn-BC, (c) Zr-BC, (d) BC, (e) AC.

Characterization of the modified biochars

3.2.1 Basic characteristics. The main properties of the modified biochars, BC and AC are listed in Table 1. The yield rates of Cs-BC, Zn-BC and Zr-BC were 33.60%, 34.01%, and 31.25% respectively, which are slightly higher than that of BC (27.46%), indicating that biomass pretreated with chemicals reduced the degradation of biomass during pyrolysis process, which is similar to the results reported by Namasivayam and Sangeetha.⁹ As biochar generally carried various surface functional groups (mainly oxygen containing groups, *e.g.* carboxylate, $-\text{COOH}$; and hydroxyl, $-\text{OH}$),⁵⁷ high amounts of elements

might result more functional groups existed on biochar's surface. The ash contents of Cs-BC and Zn-BC were significantly lower than that of BC, but their yield rates increased after modification. These results indicated that Cs-BC and Zn-BC might retain more functional groups, which was confirmed by their higher amounts of elements. In contrast, the ash content of Zr-BC was retained almost completely, indicating that very little Zr evaporated into the liquid tar and the gas phase.

The C, N, O and H contents in the biochars were higher than those in AC, as shown in Table 1. The total amounts of C, N, O, and H elements in Cs-BC and Zn-BC accounted for over 80% of

the dry weight, indicating that the effectiveness of acid washing during the preparation process. The contents of C in Cs-BC and Zn-BC were slightly higher than those in BC, whereas the amounts of H, O, and N in Zn-BC were slightly lower than those in BC. For Zr-BC, the contents of residual C, H, and N were 40.15%, 1.45%, and 0.86%, respectively, which were lower than those in BC. A contrary tendency was observed for the content of O in Zr-BC, as the oxygen in $Zr(SO_4)_2$ remained throughout the pyrolysis. The H/C ratio is an indicator for the degree of carbonization and the aromaticity of biochars. The H/C ratios of the modified biochars were lower than 0.2, indicating that the modified biochars were highly carbonized and aromatized during the pyrolysis process. The O/C and (N + O)/C ratios can be used to estimate biochar polarity. The O/C ratios of Cs-BC and BC were 0.127 and 0.111, respectively, which are similar to that of AC (0.157), suggesting that these biochars and AC had similar compositions and lower polarities. The O content of Zr-BC was 13.34% after modification with Zr(IV), whereas the C content slightly decreased, thus resulting in an increase in O/C and (N + O)/C, which indicated that Zr-BC should be more hydrophilic. The values of H/C and O/C for the modified biochars were lower than 1, suggesting significant oxygen and aliphatic hydrogen loss during the pyrolysis with the occurrence of dehydrative polycondensation and dehydrogenative polymerization.³⁷ The molar (N + O)/C ratios of Zn-BC were lowest among the biochars, suggesting that the surface of the biochars become less hydrophilic after modification with Zn(II).

Zr-BC and BC were alkaline with average pH values of 10.51 and 9.49, respectively. Nearly all zirconium oxides were maintained in Zr-BC, thus, resulting in these alkaline matter. However, the pH values of Cs-BC (7.06) and Zn-BC (6.64) were neutral in comparison to that of AC (7.42), because of the acid washing during the preparation process. As the pH_{PZC} is the pH at which the surface charge of biochar is zero, it can be used to express whether the adsorbent surface is acidic or alkaline. At a pH above the pH_{PZC} , the adsorbent surface is negatively charged, which favours the adsorption of cations; whereas at a pH below the pH_{PZC} , the surface charge of an adsorbent is positive, favouring the adsorption of anions. The pH_{PZC} values of Zr-BC and BC were 10.03, and 9.25, respectively, which indicated that their surface charges were positive when the solution was acidic, neutral, or even weakly alkaline; thus, they could attract anions. The pH_{PZC} value of BC was 9.25, but was lower at 6.89 and 6.53, for Cs-BC and Zn-BC, respectively (Table 1). These pH_{PZC} values meant that CS pretreated with CsCl and Zn(II) led to the negatively charged surfaces of Cs-BC and Zn-BC, respectively, because of the dissociation of carboxyl functional groups. The IECs of Cs-BC and Zr-BC were increased by 2.33 and 2.74 times, respectively, over BC (86.51 cmol kg⁻¹), with the exception of Zn-BC (54.18 cmol kg⁻¹). The IEC of Cs-BC (237.26 cmol kg⁻¹) was highest among all the biochars, which may be because that CS was pretreated with weakly hydrated cations (K⁺, Cs⁺).³⁸⁻⁴⁰

3.2.2 Surface characteristics and micro morphology. The microstructure properties of the modified biochars, BC and AC, including pore characteristics and specific surface area, are summarized in Table 2. The BET surface areas of Cs-BC, Zn-BC

and Zr-BC were 108.31, 150.36 and 85.58 m² g⁻¹, respectively, much higher than that of BC (27.45 m² g⁻¹), which is possibly in consequence of enhanced adsorption of N₂ in broad mesopores and micropores. However, the specific surface area of AC (735.63 m² g⁻¹, as measured in this work) was significantly larger than that of the biochars. As shown in Fig. 4a, rapid increases of the N₂ adsorption isotherm of Cs-BC and Zn-BC were observed in the low relative pressure region, where adsorption occurred within micropores. The N₂ adsorption amount of AC was significantly greater than that of the biochars. However, the pore size was similarly distributed.

The peak positions of the pore size distribution for the different modified biochars were similar, and the pore diameter was approximately below 3.80 nm (Fig. 4b). The N₂ adsorption-desorption isotherms of all the adsorbents corresponded to a similar Type IV isotherm and Type H4 hysteresis loop behaviour.⁴¹ This similarity indicated that the pores of AC and the biochars were mainly mesopores and micropores, which is similar to mesoporous industrial adsorbents. It shows that the chemicals and impregnation methods used are the most

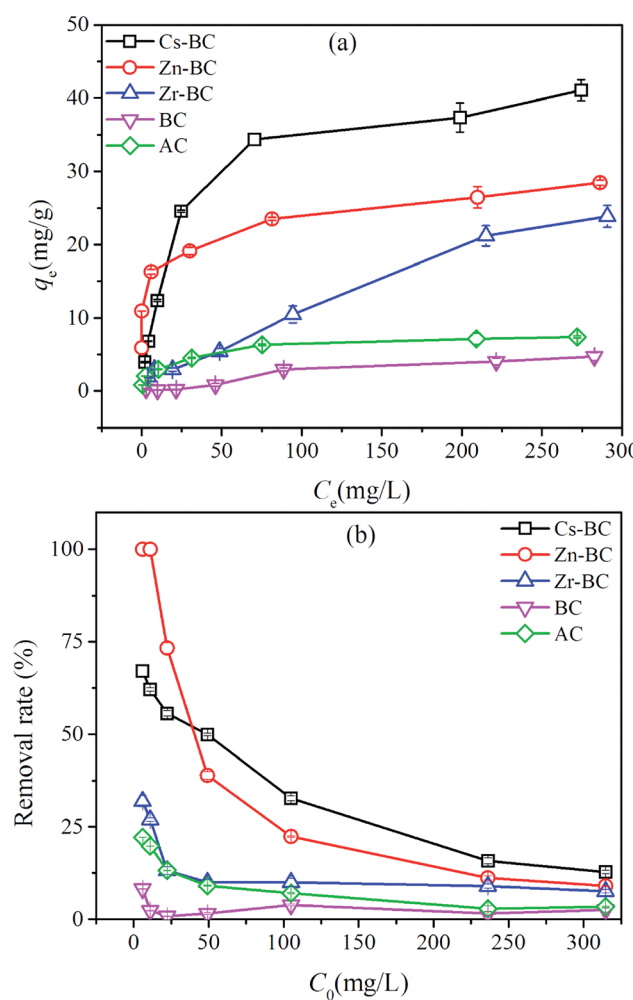


Fig. 6 Adsorption capacity (a) and removal efficiency (b) of vanadium(V) onto the modified biochars, BC, and AC. Equilibrium conditions: adsorbent dosage, 1–4 g L⁻¹; 25.0 ± 1.0 °C.



Table 3 Comparison of the maximum adsorption capacity Q_{\max} (mg g⁻¹) of various materials

| Materials | Q_{\max} (mg g ⁻¹) | Experiment condition | Ref. |
|---|--|--|--------------|
| CsCl-modified biochar (Cs-BC), Zn(II)-modified biochar (Zn-BC), Zr(IV)-modified biochar (Zr-BC) | 41.07(Cs-BC), 28.46 (Zn-BC), 23.84(Zr-BC) | 25 °C, 1 g L ⁻¹ absorbents, 5–250 mg L ⁻¹ vanadium(v) | Present work |
| 52–57% Fe(OH) ₃ and β-FeOOH (GFH), 90% FeOOH (E-33) and TiO ₂ (GTO) | 107.80 (GFH), 48.50 (GTO), 25.20(E-33) | Room temperature, 1–2 g L ⁻¹ absorbents, 1–250 mg L ⁻¹ vanadium(v) | 11 |
| Carbon cloth | 0.61 | Room temperature, 1.5 g L ⁻¹ absorbents | 44 |
| Water treatment sludge (WTS), BF slag, bauxite and sand | 13.02 (WTS), 3.62 (bauxite), 4.23 (BF slag), 4.33 (sand) | Room temperature, 10 g L ⁻¹ absorbents, 1–320 mg L ⁻¹ vanadium(v) | 45 |
| Amine-functionalized poly-grafted tamarind fruit shell | 45.86 | 30 °C, 2 g L ⁻¹ absorbents, 10–300 mg L ⁻¹ vanadium(v) | 46 |
| Amine-modified poly-grafted cellulose | 197.75 | 30 °C, 2 g L ⁻¹ , 25–600 mg L ⁻¹ vanadium(v) | 47 |
| Calcined Mg/Al hydrotalcite | 198 | 25 °C, 0.2 g L ⁻¹ , initial pH 3.0, 10–50 mg L ⁻¹ vanadium(v) | 48 |
| ZnCl ₂ activated carbon | 24.9 | 35 °C, 4 g L ⁻¹ , initial pH 4.0, 20–100 mg L ⁻¹ vanadium(v) | 9 |
| Aluminum-pillared bentonite | 24.16 | 30 °C, 1 g L ⁻¹ , initial pH 5.0, 5–400 mg L ⁻¹ vanadium(v) | 49 |
| Zr(IV)-impregnated collagen fiber | 97.81 | 30 °C, 1 g L ⁻¹ , initial pH 5.0, 101–306 mg L ⁻¹ vanadium(v) | 34 |
| Zr(IV)-loaded orange juice residue | 51.09 | 25 °C, 2 g L ⁻¹ , initial pH 2.5 | 13 |
| Protonated chitosan flakes | 2.58 | 30 °C, 5 g L ⁻¹ , initial pH 6.0, 1–5.5 mg L ⁻¹ vanadium(v) | 50 |
| Metal sludge | 24.8 | 25 °C, 2 g L ⁻¹ , initial pH 5.4, 7.6–48.4 mg L ⁻¹ vanadium(v) | 51 |
| Crosslinked chitosan | 6.27 | Room temperature, 25 °C, 0.6 g L ⁻¹ , initial pH 4.0 | 52 |

important factors that affect the types of porosity of the resulting char.

SEM images of all the absorbents were obtained at magnitude 3000 \times and were shown in Fig. 5. The surface morphologies of the absorbents were significantly different. The surface of BC was relatively smoother and had less cracks and pores than that of the modified biochars prepared under the optimized conditions. The SEM images of Cs-BC and Zn-BC showed that a large number of pores were found in Cs-BC (Fig. 5a) and Zn-BC (Fig. 5b), but their surface morphologies are significantly different. As represented in Fig. 5a, the surface of Cs-BC was moderately smooth and had obvious porous structures. However, the Zn-BC surface (Fig. 5b) was abundant with cavities and considerably irregular because of impregnation. In addition, the sizes and shapes of the pores differed, resulting in the enhanced specific surface area and vanadium(v) adsorption capacity. After Zn(II) impregnation and activation at 700 °C under N₂ atmosphere, the biochar surface became rough and many pores developed (Fig. 5b). Zn(II) impregnation may have significantly increased the generation of mesopores and specific surface area.^{25,26} The Zn(II) loaded onto CS homogeneously occupied the volume and inhibited the contraction of the particle during the carbonization, which resulted to a porous structure after it was washed with acid solution, thus producing Zn-BC with a greater specific surface area. As shown in Fig. 5c, Zr(IV) was equally loaded onto CS without pile of Zr(IV) salt

precipitation. The SEM image of Zr-BC clearly showed the enhanced surface heterogeneity of BC.

Adsorption behaviours

3.3.1 Adsorption capacities and removal efficiencies. As shown in Fig. 6a, the vanadium(v) adsorption isotherms were conducted at diverse initial concentrations of vanadium(v) solution, *i.e.* in the range of 5–200 mg L⁻¹. The maximum adsorption capacities of vanadium(v) onto Cs-BC, Zn-BC, Zr-BC, BC and AC at equilibrium were 41.07 mg g⁻¹, 28.46 mg g⁻¹, 23.84 mg g⁻¹, 4.71 mg g⁻¹ and 7.40 mg g⁻¹, respectively. Thus, the modified biochars were approximately 4.06–7.72 times more effective than BC was, probably due to their higher IECs and enhanced specific surface areas. The driving force of the

Table 4 Langmuir and Freundlich parameters for vanadium(v) adsorption onto the modified biochars, BC, and AC

| Isotherm parameter | Freundlich | | | Langmuir | | |
|--------------------|------------|-------|-------|------------|--------|-------|
| | K_F | $1/n$ | R^2 | Q_{\max} | K_L | R^2 |
| Cs-BC | 6.75 | 0.33 | 0.92 | 43.28 | 0.048 | 0.99 |
| Zn-BC | 12.05 | 0.15 | 0.62 | 26.26 | 0.21 | 0.56 |
| Zr-BC | 0.37 | 0.74 | 0.99 | 58.74 | 0.0024 | 0.98 |
| BC | 0.073 | 0.74 | 0.94 | 9.42 | 0.0036 | 0.96 |
| AC | 1.69 | 0.27 | 0.97 | 7.58 | 0.066 | 0.95 |



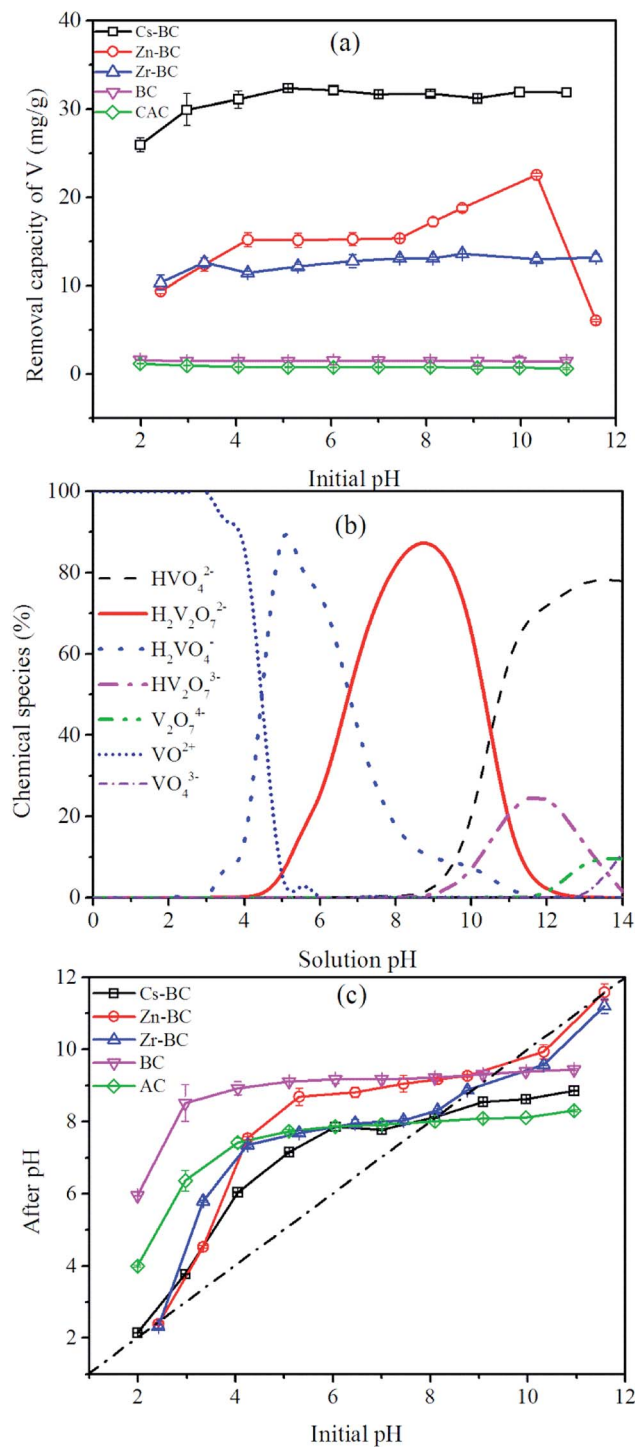
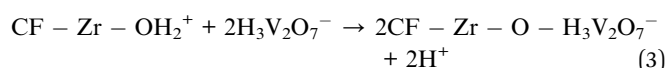


Fig. 7 Effect of pH on vanadium(v) adsorption by modified biochars, BC, and AC. (a) Effect of pH on adsorption capacity. (b) Metal ion species in aqueous solution for vanadium(v) (calculated by using Visual MINEQL ver. 3.0, $C_0 = 50 \text{ mg L}^{-1}$). (c) pH of the aqueous solution before and after vanadium(v) adsorption.

concentration gradient decreased at lower concentrations, resulting in the decrease in adsorption of vanadium(v) onto Cs-BC. The average removal efficiencies of vanadium(v) were 66% for Cs-BC, 100% for Zn-BC, and 28% for Zr-BC in the concentration range of 5–10 mg L⁻¹, respectively. For this low

concentration range, as Zn-BC and Cs-BC showed high vanadium(v) removal efficiencies, they can be used as PRB filling materials to remove vanadium(v) from contaminated groundwater. The solution pH showed a decrease for the modified biochars treatment as the initial concentration increased (Fig. S2†) after adsorption with vanadium(v). The release of H⁺ during the adsorption process can explain these results.^{42,43} Therefore, the adsorption mechanism of the modified biochars might be ion exchange.

To evaluate the efficiency of the modified biochars for the removal of vanadium(v) from aqueous solution, the adsorption capacities of the modified biochars were compared with those of other absorbents used in previous investigations (Table 3).^{11,13,34,44–52} Among these absorbents, the adsorption capacities of modified biochars for vanadium(v) were moderate (23.84 mg g⁻¹ to 41.07 mg g⁻¹), as they were lower than those of amine-modified poly-grafted cellulose (197.75 mg g⁻¹), calcined Mg/Al hydroxide (198 mg g⁻¹), Zr(iv)-impregnated collagen fiber (ZrICF) (97.81 mg g⁻¹), and GFH (107.80 mg g⁻¹). In particularly, the Zr(iv) loading content of the impregnated collagen fiber (CF) was 6.667 mmol g⁻¹, 5.29 times that of Zr-BC. Consequently, the adsorption capacity of ZrICF was 4.78 times higher than that of Zr-BC. The higher the Zr(iv) loading content is, the higher the adsorption capacity will be. Additionally, the main adsorption mechanism of vanadium(v) adsorption onto ZrICF could be ion exchange,³³ which can be described by eqn (3):



These results proved that the adsorption mechanism of Zr-BC is ion exchange. The modified biochars used in this study were developed from CS, which is a common agricultural waste. This method to prepare the modified biochars with higher adsorption capacity is relatively simple. Therefore, these modified biochars can be used as efficient absorbents to remove vanadium(v) from aqueous solution.

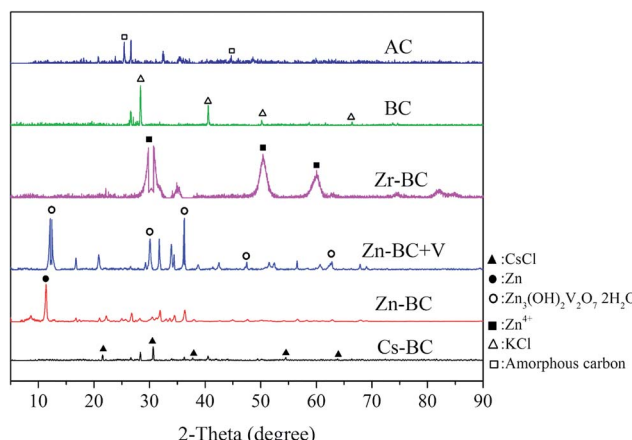


Fig. 8 XRD patterns of the modified biochars, BC, AC, and Zn-BC + V (Zn-BC after treatment with vanadium(v)). (▲: CsCl, ●: zinc carbides and zinc oxide, ○: Zn₃(OH)₂V₂O₇·2H₂O, ■: Zr⁴⁺, △: KCl, □: amorphous carbon).

3.3.2 Adsorption isotherms. The adsorption equilibrium data were further fitted by the Freundlich and Langmuir adsorption isotherm models, as presented in eqn (4) and (5), respectively:

$$q_e = K_F C_e^{1/n} \quad (4)$$

$$q_e = \frac{Q_{\max} K_L C_e}{1 + K_L C_e} \quad (5)$$

where K_F and $1/n$ are the Freundlich isotherm constant and a measure of the adsorption intensity, respectively. Q_{\max} (mg g⁻¹) and K_L (L mg⁻¹) are the theoretical maximum adsorption capacity of the adsorbent and the Langmuir isotherm constant involved to the adsorption energy, respectively.

The adsorption constants and correlation coefficients for vanadium(v) onto the biochars and AC acquired from the Freundlich and Langmuir isotherms were showed in Table 4. Excluding Zn-BC, Zr-BC and AC, the adsorption equilibrium data fit the Langmuir model better than the Freundlich model, which was confirmed *via* correlation coefficients ($R^2 = 0.84\text{--}0.99$ for the Langmuir model *versus* $0.87\text{--}0.99$ for the Freundlich model), suggesting that vanadium(v) sorption onto the Cs-BC and BC was a monolayer coverage. This result suggested that the monolayer surface adsorption took place, because of homogeneously distributed adsorption sites over the surfaces of Cs-BC and BC. However, the isotherm model used to fit the adsorption equilibrium data was solely a mathematical model;

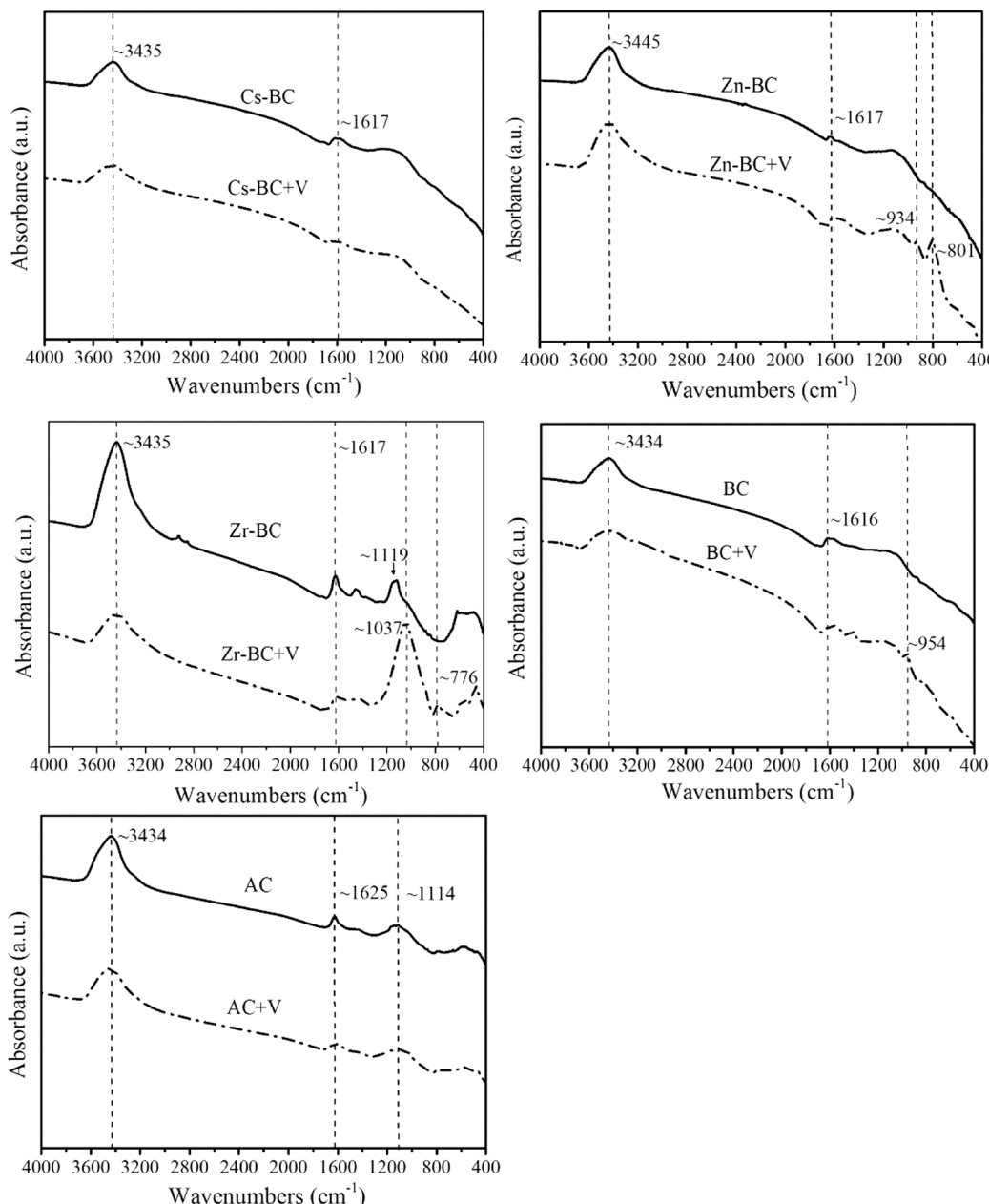


Fig. 9 FTIR spectra of the absorbents before and after treatment with vanadium(v) (absorbent + V represents an absorbent after treatment with vanadium(v)).



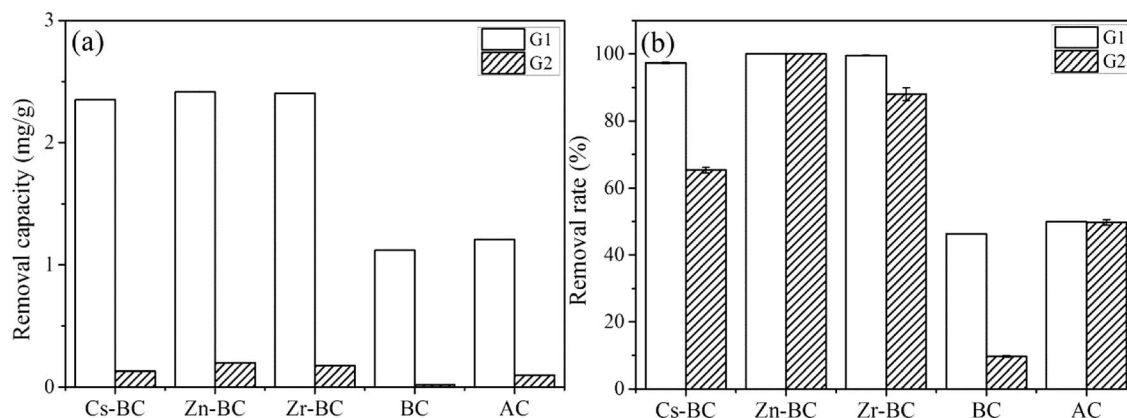


Fig. 10 Modified biochars in application of treating real contaminated groundwaters (groundwater from a vanadium tailings site (G1) and groundwater near the Chaobei River (G2)) in the Chaobei River catchment: (a) removal efficiency of vanadium(v); (b) removal capacity of vanadium(v). Equilibrium conditions: adsorbent dosage 8 g L⁻¹, 25.0 ± 1.0 °C.

it could not provide strong evidence of the actual adsorption mechanism involved in the vanadium(v) adsorption. The maximum adsorption capacity (Q_{\max}) is an important parameter for optimal design of sorption system. The maximum adsorption capacities obtained from the Langmuir equation were 43.28, 26.26, 58.74, 9.42 and 7.58 mg g⁻¹ for Cs-BC, Zn-BC, Zr-BC, BC, and AC, respectively.

3.3.3 Effect of pH. The influence of pH on the adsorption of vanadium(v) anions onto different adsorbents is shown in Fig. 7. The pH of the solution strongly impacted the adsorption interaction between metal anions and adsorbents at liquid-solid interfaces. Fig. 7a shows the influence of pH (2–11) on the adsorption process with 25 mL of vanadium(v) solution (50 mg L⁻¹) and 25 mg adsorbent. The removal capacity of vanadium(v) by Zn-BC showed a strong dependence on pH, as compared with the other adsorbents.

Vanadium(v) can exist in different forms in aqueous systems, according to the speciation diagram for vanadium. As shown in Fig. 7b, the stable vanadium species in solution can be divided into cationic (VO^{2+}) and monoanionic or polyanionic (VO_3^{3-} , VO_3^- , HVO_4^{2-} , H_2VO_4^- , $\text{HV}_2\text{O}_7^{3-}$, $\text{H}_2\text{V}_2\text{O}_7^{2-}$, $\text{HV}_2\text{O}_7^{3-}$ and $\text{V}_2\text{O}_7^{4-}$) species. Among these species, the dominant species of vanadium(v) in aqueous solution strongly depends on the pH. As shown in Fig. 7b, in pH values ranging from 2.0 to 4.0, VO^{2+} ions mainly existed as the predominant form in equilibrium. The pH_{PZC} of all the adsorbents was above 6.5, which implied that the outer surface charge of the adsorbents was positive at lower pH. The adsorption capacity of vanadium(v) onto the adsorbents decreased at pH below 4.0, possibly because of the existence of VO^{2+} cations. Electrostatic repulsion existed between the adsorbents and cationic VO^{2+} . In the pH range of 4.0–10.0, H_2VO_4^- and $\text{H}_2\text{V}_2\text{O}_7^{2-}$ ions mainly existed in equilibrium, experiencing electrostatic attraction from the positively charged adsorbents, and the dominant form shifted to HVO_4^{2-} as the pH increased. The adsorption capacities of Cs-BC, Zn-BC and Zr-BC increased at pH values ranging from 4.0 to 7.0, possibly because of the electrostatic attraction between the positively charged surface of the adsorbents and the

vanadium(v) anions. However, at pH values above the pH_{PZC} of Zn-BC, the adsorption capacity of Zn-BC continued to increase. This increase may be due to surface precipitation between zinc carbides and zinc oxide on the Zn-BC surface and HVO_4^{2-} .⁵³ The vanadium(v) adsorption onto Zn-BC at pH = 11 significantly decreased, possibly because of competition between vanadium anions and OH^- for effective adsorption sites. Additionally, leaching of Cs(I), Zn(II), and Zr(IV) from the modified biochars was measured via ICP-OES during the adsorption processes. Results showed no observable leaching of heavy metals if the solution pH was above 2.0.

3.3.4 Adsorption mechanisms. Generally, the possible adsorption mechanisms of heavy metals included several kinds of interactions, such as ion-exchange, pore filling, surface precipitation and/or complexation of metal anions, and electrostatic attraction.⁵⁷

The XRD patterns of all the adsorbents were determined in order to analyse the crystalline nature of the materials. As displayed in Fig. 8, the peaks of Cs-BC were keen-edged at 21.5° (100), 30.6° (110), 37.7° (111), 54.5° (211), and 63.8° (220), suggesting limited noise and coincidence with the phase of CsCl. Zn-BC demonstrated higher intensity of diffraction peaks, suggesting that the bulk phase changes might be induced with the Zn(II) on Zn-BC. The XRD pattern of Zn-BC shows a sharp peak at $2\theta = 11.4^\circ$ (003), which was caused by the existence of zinc carbides and zinc oxide on the Zn-BC surface. The diffraction peak of Zn-BC is sharp, indicating that the zinc loaded on Zn-BC was considerably large, though in the micro range. Furthermore, the peaks of Zn-BC + V were keen-edged at 12.3° (001), 20.8° (011), 30.1° (012), 36.2° (021), 47.5° (121), and 62.8° (221), showing limited noise and coincidence with the phase of $\text{Zn}_3(\text{OH})_2\text{V}_2\text{O}_7 \cdot 2\text{H}_2\text{O}$.⁵³ These peaks also indicated surface complexation between Zn-BC and vanadium(v). The peaks of Zr-BC shifted to $2\theta = 29.7^\circ$ (003), 49.8° (110), and 59.0° (015). This shift was possibly a result of the high absorption of X-ray by Zr(IV), compared to the carbon, oxygen and other elements in CS. The crystal structure of the cellulose in BC disappeared after carbonization. The peaks of BC were keen-



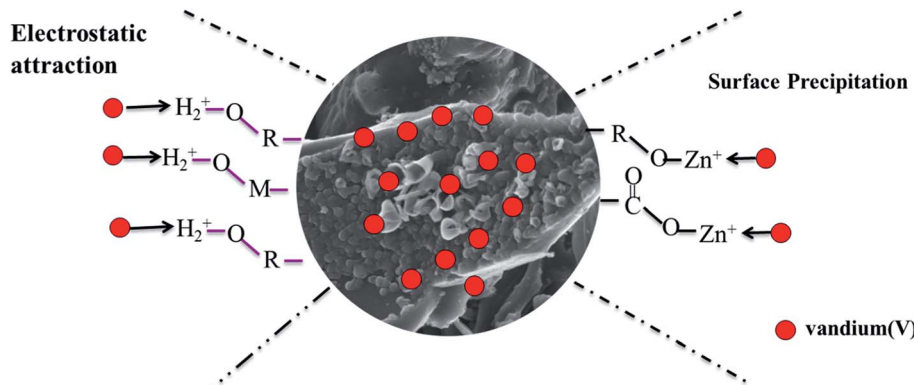


Fig. 11 Adsorption mechanism of vanadium(V) onto Zn-BC.

edged at 28.4° (200), 40.5° (220), 50.2° (222), and 66.4° (420), suggesting limited noise and coincidence with the phase of KCl, because of the potash that is widely used in agriculture. Peaks of AC were keen-edged at 26.6° (003), 43.5° (101), 54.7° (006), and 56.9° (104), showing limited noise and coincidence with the phase of carbon.

FTIR analysis was applied to identify the surface functional groups of the adsorbents. The FTIR spectra of the adsorbents and adsorbents + V (after vanadium(V) adsorption onto the adsorbents) are summarized in Fig. 9. The FTIR spectra of all the adsorbents exhibited broad peaks at $3434\text{--}3445\text{ cm}^{-1}$, which might be a result of the stack of C-H, O-H, and N-H stretching vibrations. The FTIR spectra of the biochars showed a peak at the wave number $1615\text{--}1617\text{ cm}^{-1}$, which was related to the carbonyl group C=O and the C=C in aldehyde, acetyl, ketone, and ester derivatives. The peak at $1030\text{--}1663\text{ cm}^{-1}$ was related to lignin. Therefore, the adsorbents used in this study had abundant functional groups, including C-H, O-H, N-H, and C=O, which can have strong interactions with vanadium(V) such as electrostatic attraction, ion-exchange and surface complexation.

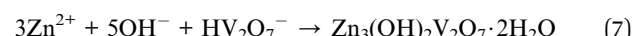
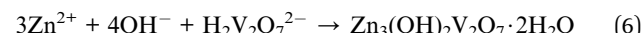
The functional groups of Zn-BC, BC and AC changed significantly after vanadium(V) sorption (Fig. 9). The broad peak observed at $3434\text{--}3445\text{ cm}^{-1}$ in the adsorbents became weak

Table 5 Anions and cations in contaminated groundwaters (groundwater from a vanadium tailings site (G1) and groundwater near the Chaobei River (G2)) of the Chaobei River catchment^a

| Anions | | Cations | | | |
|--------------------|-------|---------|----------------------------------|--------|--------|
| G1 | G2 | G1 | G2 | | |
| NO_3^- | 7.38 | 15.72 | $\text{Fe}^{2+}, \text{Fe}^{3+}$ | 0.43 | 0.44 |
| NO_2^- | 0.96 | 1.02 | K^+ | 6.38 | 22.70 |
| F^- | — | — | Ca^{2+} | 394.73 | 394.87 |
| Cl^- | 1.25 | 1.43 | Mg^{2+} | 42.46 | 30.87 |
| Br^- | 1.08 | 0.67 | Na^+ | 177.24 | 319.98 |
| SO_4^{2-} | 84.32 | 78.15 | Zn^{2+} | — | — |
| V(V) | 9.66 | 0.78 | Al^{3+} | — | — |

^a Anions and cations in contaminated groundwaters (groundwater from a vanadium tailings site (G1) and groundwater near the Chaobei River (G2)) of the Chaobei River catchment.

after vanadium(V) sorption. These changes showed that carboxylate and hydroxyl groups might be predominant functional groups for the removal of vanadium(V). The peaks at $800\text{--}1000\text{ cm}^{-1}$ that appeared in Zn-BC and BC were assigned to V_2O_5 .⁵⁴ These results suggest that electrostatic attraction was one of the adsorption mechanism of Zn-BC and BC, as the negatively charged vanadium(V) species were migrated to the positively charged surfaces of biochar with the help of electrostatic driving forces. In addition, a mixed vanadium iron oxide compound ($\text{Zn}_3(\text{OH})_2\text{V}_2\text{O}_7 \cdot 2\text{H}_2\text{O}$) resulting from the coprecipitation of vanadium(V) and Zn(II) was also observed by XRD pattern (Zn-BC + V). The reactions between vanadium(V) and Zn(II) can be described by eqn (6) and (7). Therefore, the adsorption mechanism of Zn-BC was surface precipitation and electrostatic attraction (as shown in Fig. 11). These results were in accordance with those of other reports.^{55,56}



The biochars were acquired from carbon-rich CS with abundant functional groups, including carboxylic, hydroxyl and phenolic groups (Fig. 9). Modification of the biochars enhanced the specific surface areas and IECs, which facilitated rapid mass transfer of heavy metals into the biochar pores and increased the contact between adsorption-active sites and metal molecules.⁴² As shown in Fig. S3,† the pH values of aqueous solution changed after vanadium(V) adsorption, which was in

Table 6 Costs of the modified biochars, BC, and AC. Feedstock, reagent, electricity, and labour costs were the price to treat a unit mass of 1 mg L^{-1} vanadium solution (\$/t)

| Item | Cs-BC | Zn-BC | Zr-BC | BC | AC |
|-----------------------|-------|-------|-------|-----|-----|
| Feedstock (\$/t) | 4 | 5 | 7 | 40 | — |
| Reagent (\$/t) | 32 | 44 | 56 | — | — |
| Electricity (\$/t) | 11 | 15 | 20 | 113 | — |
| Labour (\$/t) | 11 | 16 | 21 | 121 | — |
| Absorbent dosage (kg) | 24 | 35 | 42 | 212 | 135 |
| Treatment cost (\$/t) | 57 | 87 | 104 | 274 | 143 |



accordance with the hypothesis, because the release of some H^+ might occur after heavy metal adsorption onto the adsorbent surfaces, resulting in a decrease in the pH of the solution.^{42,43} The solution pH after vanadium(v) adsorption onto Cs-BC significantly dropped, clearly indicating that efficient adsorption of vanadium(v) onto Cs-BC caused more H^+ ions from the adsorption-active sites of Cs-BC to be released into the aqueous solution. Additionally, the solution pH after vanadium(v) adsorption onto Zr-BC decreased as the initial concentration of vanadium(v) increased. This result was consistent with observations reported by Liao *et al.*³⁴ Thus, the adsorption mechanism of vanadium(v) onto Cs-BC and Zr-BC was ion exchange.

Modified biochars in application of treating contaminated groundwater from the catchment of the Chaobei River.

To investigate the efficiency of the modified biochars on removal of vanadium(v) in a real case, these absorbents were used to treat the vanadium(v)-contaminated groundwaters in the catchment of the Chaobei River (groundwater from a vanadium tailings site (G1) and groundwater near the Chaobei River (G2)) (Fig. 10). The concentrations of vanadium(v) in G1 and G2 as the unknown samples were measured as 9.66 mg L^{-1} and 0.78 mg L^{-1} , respectively (Table 5). It is clearly seen from Fig. 10 that the modified biochars used to treat real contaminated water significantly differed, at a dose of 4 g L^{-1} . The removal efficiencies of vanadium(v) in G1 on modified biochars had reached 92%, however, these of vanadium(v) in groundwater were reflected by the following sequence: Zn-BC (100%) > Zr-BC (88.03%) > Cs-BC (65.42%) > AC (49.74%) > BC (9.67%), which is different from the adsorption isotherm. As shown in Table 5, the main ions that existed in G1 and G2 were SO_4^{2-} , NO_3^- , Ca^{2+} , Na^+ , and K^+ . The concentrations of NO_3^- and Na^+ in G2 were almost twofold than those in G1. Ion exchange was the main adsorption mechanism of Cs-BC in previous analysis, resulting the low removal efficiency in G2. As the main adsorption mechanism of Zn-BC is surface precipitation and electrostatic attraction, this biochar still can effectively remove vanadium from groundwater in the presence of high concentrations of competing ions (SO_4^{2-} and NO_3^-), indicating that the selectivity of the biochar was improved by the modification of Zn(II).

Economic costs were analysed to evaluate the economic feasibility of the modified biochars. The total costs of the modified biochars and BC mainly comprise feedstock, reagents, electricity, and labour costs, which was the price to treat a unit mass of 1 mg L^{-1} vanadium solution (\$/t), and are listed in Table 6. The reagent use for the modification of the biochar was the major contributor to the total cost of the modified biochar production, comprising 55% (\$32/t) in Cs-BC, 55% (\$44/t) in Zn-BC, and 54% (\$56/t) in Zr-BC (Table 6). The production costs for the modified biochars to treat a unit mass of 1 mg L^{-1} vanadium solution ranged from \$57/t to \$104/t, which were lower than that for AC (\$143/t), owing to its lower removal capacity. In conclusion, Zn-BC can be used as a low-cost PRB filling material for the efficient removal of vanadium(v) from real contaminated water.

Conclusion

The results of this study showed that Zn-BC could efficiently remove vanadium(v) from real contaminated groundwater in the catchment of the Chaobei River.

(1) The BET surface areas of Cs-BC, Zn-BC, and Zr-BC were 108.314 , 150.356 , and $85.579\text{ m}^2\text{ g}^{-1}$, higher by 3.12–5.48 times, compared to the $27.448\text{ m}^2\text{ g}^{-1}$ for BC.

(2) Cs-BC, Zn-BC, and Zr-BC exhibited excellent adsorption performances without depending on pH (4.0–8.0). The adsorption capacities of these biochars were 41.07 , 28.46 , and 23.84 mg g^{-1} , respectively, which were much higher than BC (4.71 mg g^{-1}) and AC (7.40 mg g^{-1}), according to the Langmuir isotherm model. In addition, no heavy metals leached from the modified biochars if the solution pH was above 2.0.

(3) The main adsorption mechanism onto Cs-BC and Zr-BC was ion exchange, whereas the adsorption mechanism for Zn-BC was surface precipitation and electrostatic attraction, according to FTIR and XRD analysis.

(4) As the removal efficiencies of vanadium(v) in the real contaminated groundwaters (G1 and G2) by Zn-BC had reached 100%, Zn-BC can be used as a PRB filling material for the efficient removal of vanadium(v).

Conflicts of interest

There are no conflicts to declare.

Acknowledgements

This study was supported by the Major Science and Technology Program for Water Pollution Control and Treatment (2015ZX07205-003) and Tsinghua University-Laboratory for Solid Waste Management and Environment Safety.

References

- 1 J. Xudong and T. Yanguo, Techniques on soil remediation and disposal of vanadium pollution, *Chin. J. Soil Sci.*, 2008, **39**(02), 448–452.
- 2 Z. Lichun, *et al.* The distribution and influence factors of species vanadium in shallow groundwater near the slag field of Baguan river in Panzhihua area, *Wutan Huatan Jisuan Jishu*, 2015, **37**(02), 263–266.
- 3 Z. Licheng and Z. Kezhun, Background values of trace elements in the source area of the Yangtze River, *Sci. Total Environ.*, 1992, **125**, 391–404.
- 4 D. A. Li, *et al.* Soil heavy metal contamination related to roasted stone coal slag: a study based on geostatistical and multivariate analyses, *Environ. Sci. Pollut. Res.*, 2016, **23**(14), 14405–14413.
- 5 California Department Of Public Health-DrinkingWater Program, California Department of Public Health-Drinking Water Program.
- 6 C. Kantar, *et al.* Cr(VI) removal from aqueous systems using pyrite as the reducing agent: Batch, spectroscopic and column experiments, *J. Contam. Hydrol.*, 2015, **174**, 28–38.



7 F. Obiri-Nyarko, *et al.* Geochemical modelling for predicting the long-term performance of zeolite-PRB to treat lead contaminated groundwater, *J. Contam. Hydrol.*, 2015, **177-178**, 76-84.

8 W. Han, *et al.* Studies on the optimum conditions using acid-washed zero-valent iron/aluminum mixtures in permeable reactive barriers for the removal of different heavy metal ions from wastewater, *J. Hazard. Mater.*, 2016, **302**, 437-446.

9 C. Namasivayam and D. Sangeetha, Removal and recovery of vanadium(V) by adsorption onto $ZnCl_2$ activated carbon: Kinetics and isotherms, *Adsorption*, 2006, **12**(2), 103-117.

10 A. Padilla-Rodríguez, *et al.* Synthesis of protonated chitosan flakes for the removal of vanadium(III, IV and V) oxyanions from aqueous solutions, *Microchem. J.*, 2015, **118**, 1-11.

11 A. Naeem and S. Mustafa, Vanadium removal by metal (hydr) oxide adsorbents, *Water Res.*, 2007, **41**(7), 1596-1602.

12 C. L. Peacock and D. M. Sherman, Vanadium(V) adsorption onto goethite (α -FeOOH) at pH 1.5 to 12: a surface complexation model based on *ab initio* molecular geometries and EXAFS spectroscopy, *Geochim. Cosmochim. Acta*, 2004, **68**(8), 1723-1733.

13 Q. Hu, *et al.* Adsorptive recovery of vanadium(V) from chromium(VI)-containing effluent by Zr(IV)-loaded orange juice residue, *Chem. Eng. J.*, 2014, **248**, 79-88.

14 S. P. Sohi, Carbon Storage with Benefits, *Science*, 2012, **338**, 1034-1035.

15 M. Chen, J. Zhao and L. Xia, Enzymatic hydrolysis of maize straw polysaccharides for the production of reducing sugars, *Carbohydr. Polym.*, 2008, **71**(3), 411-415.

16 J. Li, *et al.* Semi-continuous anaerobic co-digestion of dairy manure with three crop residues for biogas production, *Bioresour. Technol.*, 2014, **156**, 307-313.

17 D. Mohan, *et al.* Lead sorptive removal using magnetic and nonmagnetic fast pyrolysis energy cane biochars, *J. Colloid Interface Sci.*, 2015, **448**, 238-250.

18 D. Mohan, *et al.* Sorption of arsenic, cadmium, and lead by chars produced from fast pyrolysis of wood and bark during bio-oil production, *J. Colloid Interface Sci.*, 2007, **310**(1), 57-73.

19 D. Mohan, *et al.* Cadmium and lead remediation using magnetic oak wood and oak bark fast pyrolysis bio-chars, *Chem. Eng. J.*, 2014, **236**, 513-528.

20 G. Tan, *et al.* Sorption of mercury (II) and atrazine by biochar, modified biochars and biochar based activated carbon in aqueous solution, *Bioresour. Technol.*, 2016, **211**, 727-735.

21 H. Wang, *et al.* Removal of Pb(II), Cu(II), and Cd(II) from aqueous solutions by biochar derived from KMnO₄ treated hickory wood, *Bioresour. Technol.*, 2015, **197**, 356-362.

22 B. Shen, *et al.* Elemental mercury removal by the modified bio-char from medicinal residues, *Chem. Eng. J.*, 2015, **272**, 28-37.

23 A. AHMADPOUR and D. D. Do, The Preparation of Activated Carbon from Macadamia Nutshell by Chemical Activation, *Carbon*, 1997, **12**(35), 1723-1732.

24 L. Trakal, *et al.* Copper removal from aqueous solution using biochar: Effect of chemical activation, *Arabian J. Chem.*, 2014, **7**(1), 43-52.

25 A. Kumar and H. M. Jena, Adsorption of Cr(VI) from aqueous phase by high surface area activated carbon prepared by chemical activation with $ZnCl_2$, *Process Saf. Environ. Prot.*, 2017, **109**, 63-71.

26 F. Boudrahem, F. Aissani-Benissad and H. Aït-Amar, Batch sorption dynamics and equilibrium for the removal of lead ions from aqueous phase using activated carbon developed from coffee residue activated with zinc chloride, *J. Environ. Manage.*, 2009, **90**(10), 3031-3039.

27 A. Sowmya and S. Meenakshi, Zr(IV) loaded cross-linked chitosan beads with enhanced surface area for the removal of nitrate and phosphate, *Int. J. Biol. Macromol.*, 2014, **69**, 336-343.

28 T. A. H. Nguyen, *et al.* Adsorption of phosphate from aqueous solutions and sewage using zirconium loaded okara (ZLO): Fixed-bed column study, *Sci. Total Environ.*, 2015, **523**, 40-49.

29 B. K. Biswas, *et al.* Adsorptive removal of As(V) and As(III) from water by a Zr(IV)-loaded orange waste gel, *J. Hazard. Mater.*, 2008, **154**(1-3), 1066-1074.

30 L. H. Velazquez-Jimenez, J. A. Arcibar-Orozco and J. R. Rangel-Mendez, Overview of As(V) adsorption on Zr-functionalized activated carbon for aqueous streams remediation, *J. Environ. Manage.*, 2018, **212**, 121-130.

31 N. N. Das, *et al.* Adsorption of Cr(VI) and Se(IV) from their aqueous solutions onto Zr⁴⁺-substituted ZnAl/MgAl-layered double hydroxides: effect of Zr⁴⁺ substitution in the layer, *J. Colloid Interface Sci.*, 2004, **270**(1), 1-8.

32 X. Chen, *et al.* Efficient removal and environmentally benign detoxification of Cr(VI) in aqueous solutions by Zr(IV) cross-linking chitosan magnetic microspheres, *Chemosphere*, 2017, **185**, 991-1000.

33 T. Chen, *et al.* Influence of pyrolysis temperature on characteristics and heavy metal adsorptive performance of biochar derived from municipal sewage sludge, *Bioresour. Technol.*, 2014, **164**, 47-54.

34 X. Liao, *et al.* Adsorption of metal anions of vanadium(V) and chromium(VI) on Zr(IV)-impregnated collagen fiber, *Adsorption*, 2008, **14**(1), 55-64.

35 T. Mahmood, *et al.* Comparison of Different Methods for the Point of Zero Charge Determination of NiO, *Ind. Eng. Chem. Res.*, 2011, **50**(17), 10017-10023.

36 X. Hu, G. L. Lu and Y. Yang, Determination of cation-exchange capacity in clay $[Co(NH_3)_6]^{3+}$ exchange method, *Chin. J. Anal. Chem.*, 2000, **11**(28), 1402-1405.

37 P. De Filippis, *et al.* Production and Characterization of Adsorbent Materials from Sewage Sludge by Pyrolysis, *Chem. Eng. Trans.*, 2013, **32**, 205-210.

38 X. Shi, L. Ji and D. Zhu, Investigating roles of organic and inorganic soil components in sorption of polar and nonpolar aromatic compounds, *Environ. Pollut.*, 2010, **158**(1), 319-324.



39 S. A. Boyd, *et al.* Mechanisms for the Adsorption of Substituted Nitrobenzenes by Smectite Clays, *Environ. Sci. Technol.*, 2001, **35**(21), 4227–4234.

40 S. B. Haderlein, K. W. Weissmahr and R. P. Schwarzenbach, Specific Adsorption of Nitroaromatic Explosives and Pesticides to Clay Minerals, *Environ. Sci. Technol.*, 1996, **30**, 612–622.

41 K. S. W. Sing, Reporting Physisorption Data for Gas/Solid Systems with Special Reference to the Determination of Surface Area and Porosity, *Pure Appl. Chem.*, 1982, **11**(54), 2201–2218.

42 L. Trakal, *et al.* Copper removal from aqueous solution using biochar: Effect of chemical activation, *Arabian J. Chem.*, 2014, **7**(1), 43–52.

43 H. Jin, *et al.* Biochar pyrolytically produced from municipal solid wastes for aqueous As(V) removal: Adsorption property and its improvement with KOH activation, *Bioresour. Technol.*, 2014, **169**, 622–629.

44 A. Afkhami and B. E. Conway, Investigation of Removal of Cr(VI), Mo(VI), W(VI), V(IV), and V(V) Oxy-ions from Industrial Waste-Waters by Adsorption and Electrosorption at High-Area Carbon Cloth, *J. Colloid Interface Sci.*, 2002, **251**(2), 248–255.

45 T. Hua, *et al.* Potential for use of industrial waste materials as filter media for removal of Al, Mo, As, V and Ga from alkaline drainage in constructed wetlands – Adsorption studies, *Water Res.*, 2015, **71**, 32–41.

46 T. S. Anirudhan and P. G. Radhakrishnan, Adsorptive performance of an amine-functionalized poly(hydroxyethylmethacrylate)-grafted tamarind fruit shell for vanadium(V) removal from aqueous solutions, *Chem. Eng. J.*, 2010, **165**(1), 142–150.

47 T. S. Anirudhan, S. Jalajamony and L. Divya, Efficiency of Amine-Modified Poly(glycidyl methacrylate)-Grafted Cellulose in the Removal and Recovery of Vanadium(V) from Aqueous Solutions, *Ind. Eng. Chem. Res.*, 2009, **48**(4), 2118–2124.

48 T. Wang, *et al.* The influence of vanadate in calcined Mg/Al hydrotalcite synthesis on adsorption of vanadium (V) from aqueous solution, *Chem. Eng. J.*, 2012, **181–182**, 182–188.

49 D. M. Manohar, *et al.* Removal of Vanadium(IV) from Aqueous Solutions by Adsorption Process with Aluminum-Pillared Bentonite, *Ind. Eng. Chem. Res.*, 2005, **44**(17), 6676–6684.

50 A. Padilla-Rodríguez, *et al.* Synthesis of protonated chitosan flakes for the removal of vanadium(III, IV and V) oxyanions from aqueous solutions, *Microchem. J.*, 2015, **118**, 1–11.

51 A. Bhatnagar, *et al.* Vanadium removal from water by waste metal sludge and cement immobilization, *Chem. Eng. J.*, 2008, **144**(2), 197–204.

52 S. Qian, *et al.* Studies of adsorption properties of crosslinked chitosan for vanadium(V), tungsten(VI), *J. Appl. Polym. Sci.*, 2004, **92**, 1584–1588.

53 S. Ni, *et al.* Crystallized $Zn_3(OH)_2V_2O_7 \cdot nH_2O$: Hydrothermal synthesis and magnetic property, *J. Alloys Compd.*, 2009, **477**(1–2), L1–L3.

54 Y. Fan, *et al.* Separation and recovery of chromium and vanadium from vanadium-containing chromate solution by ion exchange, *Hydrometallurgy*, 2013, **136**, 31–35.

55 X. S. Wang, *et al.* Removal of Cr (VI) with wheat-residue derived black carbon: Reaction mechanism and adsorption performance, *J. Hazard. Mater.*, 2010, **175**(1–3), 816–822.

56 Z. R. Komy, *et al.* Characterisation of acidic sites of *Pseudomonas* biomass capable of binding protons and cadmium and removal of cadmium *via* biosorption, *World J. Microbiol. Biotechnol.*, 2006, **22**(9), 975–982.

57 X. Tan, *et al.* Application of biochar for the removal of pollutants from aqueous solutions, *Chemosphere*, 2015, **125**, 70–85.

